NEUROSYSTEMS

Subpopulations of cholinergic, GABAergic and glutamatergic neurons in the pedunculopontine nucleus contain calcium-binding proteins and are heterogeneously distributed

Cristina Martinez-Gonzalez,[1] Hui-Ling Wang,[2] Benjamin R. Micklem,[1] J. Paul Bolam[1] and Juan Mena-Segovia[1]

[1]Medical Research Council Anatomical Neuropharmacology Unit, Department of Pharmacology, University of Oxford, Mansfield Road, Oxford OX1 3TH, UK
[2]Intramural Research Program, Cellular Neurophysiology, Biomedical Research Center, National Institute on Drug Abuse, Baltimore, MD, USA

Abstract

Neurons in the pedunculopontine nucleus (PPN) are highly heterogeneous in their discharge properties, their neurochemical markers, their pattern of connectivity and the behavioural processes in which they participate. Three main transmitter phenotypes have been described, cholinergic, GABAergic and glutamatergic, and yet electrophysiological evidence suggests heterogeneity within these subtypes. To gain further insight into the molecular composition of these three populations in the rat, we investigated the pattern of expression of calcium binding proteins (CBPs) across distinct regions of the PPN and in relation to the presence of other neurochemical markers. Calbindin- and calretinin-positive neurons are as abundant as cholinergic neurons, and their expression follows a rostro-caudal gradient, whereas parvalbumin is expressed by a low number of neurons. We observed a high degree of expression of CBPs by GABAergic and glutamatergic neurons, with a large majority of calbindin- and calretinin-positive neurons expressing GAD or VGluT2 mRNA. Notably, CBP-positive neurons expressing GAD mRNA were more concentrated in the rostral PPN, whereas the caudal PPN was characterized by a higher density of CBP-positive neurons expressing VGluT2 mRNA. In contrast to these two large populations, in cholinergic neurons expression of calretinin is observed only in low numbers and expression of calbindin is virtually non-existent. These findings thus identify novel subtypes of cholinergic, GABAergic and glutamatergic neurons based on their expression of CBPs, and further contribute to the notion of the PPN as a highly heterogeneous structure, an attribute that is likely to underlie its functional complexity.

Introduction

The pedunculopontine nucleus (PPN) is a brainstem structure involved in a wide range of physiological and behavioural processes, including locomotion (Skinner & Garcia-Rill, 1984; Garcia-Rill *et al.*, 1987, 1990), gait control (Pahapill & Lozano, 2000), and regulation of rapid eye movement sleep and wakefulness (Steriade *et al.*, 1990). Different functional roles are associated with the anterior or posterior PPN (Inglis *et al.*, 2001; Alderson *et al.*, 2006, 2008). This subdivision is supported by the neurochemically diverse connectivity of the PPN with many structures of the brain and spinal cord (Martinez-Gonzalez *et al.*, 2011), and the heterogeneous distribution of its neuronal populations (Olszewski & Baxter, 1982; Mena-Segovia *et al.*, 2009; Wang & Morales, 2009).

The PPN is classically defined by the distribution of the Ch5-group of cholinergic neurons (Mesulam *et al.*, 1983). However, the PPN also contains other populations of neurons which are more abundant than cholinergic neurons, most notably GABAergic and glutamatergic neurons (Mena-Segovia *et al.*, 2009; Wang & Morales, 2009). Recent evidence shows that these populations are heterogeneous with respect to their *in vivo* discharge properties across different brain states and their pattern of connectivity (Mena-Segovia *et al.*, 2008a; Ros *et al.*, 2010), but it is unknown whether these differences relate to differences in their molecular composition. In addition to the markers that define these three populations of neurons, it has also been reported that the PPN contains nitric oxide synthase, NADPH diaphorase (Vincent *et al.*, 1983; Vincent & Kimura, 1992), and the calcium binding proteins (CBPs) calbindin, calretinin and parvalbumin (Coté & Parent, 1992; Dun *et al.*, 1995; Fortin & Parent, 1999). Among CBPs expressed in the brain, calbindin D_{28k} and calretinin (29 kDa) (Pochet *et al.*, 1985), members of the EF-hand family (helix E, a loop and another helix F motif) (Kretsinger & Nockolds, 1973; Camp & Wijesinghe, 2009), have been used extensively as markers to distinguish different types of neurons in distinct areas of the brain (Celio, 1990; Gulyas *et al.*, 1991; Acsady *et al.*, 1993; Parent *et al.*,

1996; Staiger *et al.*, 2004). Calbindin and calretinin have a functional role in the modulation of intracellular calcium levels by binding Ca^{2+} at different kinetic rates (Nagerl *et al.*, 2000), conferring them particular physiological and functional properties (Chard *et al.*, 1993; Schwaller *et al.*, 2002; Camp & Wijesinghe, 2009). Understanding the role of neurons expressing these markers can lead to a better understanding of the functions of the PPN, but this necessitates knowledge of their numbers, distribution and expression by neurotransmitter-specific neuronal types.

In this study, we estimated the total number and density of the calbindin- and calretinin-positive neurons found in the rostral and caudal PPN, and identified their transmitter phenotype by combining immunohistochemistry and *in situ* hybridization. We show that a large proportion of calbindin- and calretinin-positive neurons are GABAergic or glutamatergic, that they are heterogeneously distributed within the PPN and that only a minor proportion of them are cholinergic.

Materials and methods

Histology

All animal procedures used in this study were carried out under the authority of the Animals (Scientific Procedures) Act, 1986 (UK) and the University of Oxford Ethical Review Committee or the NIDA IRP local Animal Care and Use Committee. Sprague–Dawley rats (225–300 g) were used for immunohistochemical analyses. They were deeply anaesthetized using a mixture of ketamine (30 mg/kg, i.p.; Ketaset, Willow Francis, UK) and xylazine (3 mg/kg, i.p.; Rompun, Bayer, Germany) and transcardially perfused with 0.1 M phosphate-buffered saline (PBS) followed by 4% paraformaldehyde (PFA) in 0.1 M phosphate buffer (PB), pH 7.4. Brains were removed and post-fixed for 0.5–1.5 h at room temperature. Sagittal sections (50 μm thick) of the brainstem were then cut using a vibratome (Leica Microsystems, UK), collected in series of six and stored in 0.05% sodium azide in PBS. For *in situ* hybridization, Sprague–Dawley rats (280–300 g) were deeply anaesthetized with chloral hydrate (300 mg/kg), and transcardially perfused with 4% PFA in 0.1 M PB, pH 7.3. The brains were removed and post-fixed for 2 h at 4 °C and then stored at −80 °C until cryosections of 18 μm thickness were collected in series of eight.

Immunohistochemistry (IHC)

Three of the six series of sections collected for immunohistochemical analyses and containing the PPN ($n = 6$ rats) were double-immuno-labelled to reveal calbindin and choline acetyltransferase (ChAT), calretinin and ChAT, or parvalbumin and ChAT. For bright-field IHC, free-floating serial sections were blocked for 1 h in normal donkey serum (NDS; Jackson Immunoresearch Laboratories Inc., West Grove, PA, USA; 10% in 0.3% Triton X-100 in PBS) then incubated overnight at 4 °C with an antibody against ChAT raised in goat (AB144P; Chemicon, Temecula, CA, USA; 1 : 500 in 1% NDS, 0.3% Triton X-100 in PBS). The following day, the sections were washed in PBS and incubated overnight with a biotinylated donkey anti-goat secondary antibody (Vector Laboratories, Burlingame, CA, USA; 1 : 500 in 1% NDS, 0.3% Triton X-100 in PBS). After PBS washes, sections were incubated for 4–7 h at room temperature or overnight at 4 °C in avidin-biotin peroxidase complex (ABC; Vector Laboratories; prepared according to the manufacturer's instructions). Immunolabelling for ChAT was then revealed by pre-incubation for 15 min in diaminobenzidine (DAB; Sigma, St Louis, MO, USA; 0.025%, w/v, in 0.05 M Tris buffer, pH 7.4) and then in the same DAB solution

containing hydrogen peroxide (0.03%, v/v, in dH_2O; Sigma) for 5–10 min. After PBS washes, immunolabelled sections were incubated overnight at 4 °C with either an antibody raised against calbindin in mouse (CB300; Swant, Marly, Switzerland; 1 : 5000 in 1% NDS, 0.3% Triton X-100 in PBS), with an antibody raised against calretinin in rabbit (7699/3H; Swant; 1 : 5000 in 1% NDS, 0.3% Triton X-100 in PBS) or an antibody raised against parvalbumin (P3088, Clone PARV-19; Sigma; 1 : 2000 in 1% NDS, 0.3% Triton X-100 in PBS). The sections were then washed in PBS and incubated with the appropriate biotinylated donkey anti-mouse (calbindin and parvalbumin; Vector Laboratories; 1 : 500 in 1% NDS, 0.3% Triton X-100 in PBS) or biotinylated donkey anti-rabbit secondary (calretinin; Vector Laboratories; 1 : 500 in 1% NDS, 0.3% Triton X-100 in PBS). The calbindin, calretinin or parvalbumin immunolabelling was revealed by incubation of the tissue in Vector-SG substrate solution for 3–5 min at room temperature, according to the manufacturer's instructions (Vector-SG substrate kit; SK-4700). Sections were washed in PBS, mounted on gelatin-coated slides, dried and dehydrated through increasing concentrations of alcohol and then xylene, and mounted in resin (XAM; BDH Laboratory Supplies, Poole, UK).

For fluorescence IHC, triple-immunostaining for ChAT, calbindin and calretinin was performed on sections where the PPN was largest (three sections per brain, $n = 3$ rats). The primary antibodies for ChAT, calbindin and calretinin were used as described above, but the secondary antibodies were donkey anti-goat-Cy5 for ChAT labelling (Jackson Immunoresearch), donkey anti-mouse-Cy3 for calbindin labelling (Jackson Immunoresearch) and donkey anti-rabbit-Alexa-488 for calretinin labelling (Molecular Probes, Invitrogen, Paisley, UK). Sections were mounted in Vectashield (Vector Laboratories) and stored in the dark at 4 °C until use. Control reactions were performed by omitting each of the primary antibodies. In turn, the immunofluorescence of the remaining two markers was assessed, revealing complete absence of fluorescence for the omitted antibody.

Combination of in situ hybridization and IHC

Sagittal free-floating sections (18 μm in thickness) were processed as described previously (Wang & Morales, 2008, 2009). Sections were incubated for 10 min in PB containing 0.5% Triton X-100, rinsed twice for 5 min with PB, treated with 0.2 M HCl for 10 min, rinsed twice for 5 min with PB and then acetylated in 0.25% acetic anhydride in 0.1 M triethanolamine, pH 8.0, for 10 min. Sections were rinsed twice for 5 min with PB, and post-fixed with 4% paraformaldehyde for 10 min. Prior to hybridization and after a final rinse with PB, the free-floating sections were incubated in hybridization buffer (50% formamide; 10% dextran sulfate; 5 × Denhardt's solution; 0.62 M NaCl; 50 mM DTT; 10 mM EDTA; 20 mM PIPES, pH 6.8; 0.2% SDS; 250 μg/mL salmon sperm DNA; 250 μg/mL tRNA) for 2 h at 55 °C. Sections were hybridized for 16 h at 55 °C in hybridization buffer containing [^{35}S]- and [^{33}P]-labelled single-stranded antisense rat ChAT (nucleotides 271–2247, accession no. NM017464), vGluT2 (nucleotides 1704–2437; accession no. NM-053427), GAD65 (nucleotides 1–1758; accession no. NM012563) and GAD67 (nucleotides 1–1782; accession no. NM-017007), calbindin (nucleotides 26–1731; accession no. NM_031984.2) or calretinin (nucleotides 29–1547; accession no. BC087603.1) probes at 10^7 c.p.m./mL. Sections were treated with 4 μg/mL RNase A at 37 °C for 1 h, washed with 1 × standard sodium citrate (SSC), 50% formamide at 55 °C for 1 h, and with 0.1 × SSC at 68 °C for 1 h. After the last SSC wash, sections were rinsed with PB and incubated for 1 h in PB supplemented with 4% bovine serum albumin and 0.3% Triton X-100. This was followed by overnight incubation at 4 °C with a goat anti-ChAT antibody,

mouse anti-calbindin or rabbit anti-calretinin, as described above. After rinsing three times for 10 min each in PB, sections were processed by the avidin-biotin-peroxidase method with an ABC kit (Vector Laboratories). The material was incubated for 1 h at room temperature in a 1 : 200 dilution of the biotinylated secondary antibody, rinsed with PB, and incubated with ABC for 1 h. Sections were rinsed and the peroxidase reaction was then developed with 0.05% DAB and 0.03% hydrogen peroxide. Free-floating sections were mounted on gelatin-coated slides. Slides were dipped in Ilford K.5 nuclear tract emulsion (Polysciences, Inc., Warrington, UK; 1 : 1 dilution in double distilled water) and exposed in the dark at 4 °C for 4 weeks prior to development.

Image acquisition

Light microscopic images of immunolabelled neurons were captured with a DVC1310c camera (Digital Video Camera Co., Austin, TX, USA) attached to an Eclipse 80i microscope (Nikon, Surrey, UK) with NEUROLUCIDA software (MBF Bioscience, Colchester, VT, USA). Confocal microscope images were obtained with a laser scan head (LSM510; Zeiss, Welwyn Garden City, UK) mounted on an inverted microscope (Axiovert 100M; Zeiss). Stacks of 20 images were taken through the z-axis using a 40 × oil objective (Plan-Neofluar; Zeiss) and a frame of 325.8 μm (x) × 325.8 μm (y) × 1 μm (z) for each. For Alexafluor 488 the emission was selected through secondary dichroic mirrors NFS 635 VIS, then NFT 545, before passing through an LP 505 filter. For Cy3 the emission was selected through two secondary dichroic mirrors, NFS 635 VIS, then NFT 545, before passing through an LP 560 filter. For Cy5 the secondary dichroic mirror was NFS 635 VIS, then emission filter LP 650. Scanning was performed in multi-track mode with line switching (each channel was scanned in sequence for the first line of the image before the second line was scanned, i.e. all lasers/detectors were not on at the same time). The brightness and contrast of the images were subsequently adjusted in PHOTOSHOP (Adobe Systems Inc., Mountain view, CA, USA).

Cell counting

Stereological cell counts and measurements were carried out using STEREO-INVESTIGATOR software (version 8; MBF Bioscience), an Eclipse 80i microscope (Nikon) with a computer-controlled motorized stage (LUDL Electronic Products), and a Lucivid module (MBF Bioscience) projecting the computer's display into the drawing tube of the microscope.

To determine the average soma size of neurons, we measured the radii of the roughly round neurons or the greatest distances across multipolar-shaped neurons ($n = 100$ calbindin-positive neurons, $n = 100$ calretinin-positive neurons), using a 63× oil objective. The neurons used for this analysis were chosen randomly in the rostral and caudal PPN using STEREO-INVESTIGATOR software.

We studied the rostro-caudal distribution of the calbindin- and calretinin-positive neurons in the PPN using a stereological method previously described, based on the subdivision of the PPN into equally sized segments (Mena-Segovia et al., 2009). Using the centre of the substantia nigra pars reticulata (SNr) as the starting point in the sagittal plane, we drew concentric circles of 300 μm each to divide the PPN into 10 segments (S1–S10) – as a result, S1 it is the most rostral and closest to the SNr, whereas S10 is the most caudal and distal segment to the SNr (see inset to Fig. 2C below). ChAT-positive neurons were used to delimit the boundary of the PPN, using criteria consistent with previous studies (Mesulam et al., 1983; Mena-Segovia et al., 2009).

Each segment was outlined as a closed contour using the PPN boundary and concentric circles as guides with a 4× objective in STEREO-INVESTIGATOR. We used an optical fractionator with counting frame and sampling grid of 75 × 75 μm for the IHC sections. The sections were cut at 50 or 18 μm thickness (depending on the IHC or combined IHC and in situ hybridization protocol), but were typically 14 or 6–8 μm thick once processed, dehydrated and mounted. A 100× 1.4 NA oil-immersion objective was used for all cell counts for low depth of field.

A neuron was considered to be immunopositive if it was labelled by the typical brown colour of the DAB peroxidase reaction product in the cytoplasm and proximal dendrites, or the black–blue reaction product of the Vector slate-gray accordingly. The slate-gray-labelled neurons were easily differentiated from the DAB-labelled neurons (see Fig. 1) and from the neurons containing both reaction products (see Fig. 3A′). For IHC-treated sections, an immunopositive neuron was counted if the top surface of its nucleus was below the upper limit of the optical fractionator (a 2-μm guard zone was used below the top of the mounted section). If the nucleus of a cell was more than 50% outside the contour boundary, it was not counted. To estimate the total number of immunopositive neurons in the PPN, we used the following formula:

$$\frac{1}{\text{(fraction of height of section sampled)}} \times \frac{1}{\text{(fraction of sections sampled)}} \times \text{total count}$$

Cell density per segment was obtained by dividing the estimated number of neurons per segment in each animal by the total segment volume, then taking the mean across animals.

For sections processed by both in situ hybridization and IHC, we could not use an optical fractionator as the silver grains revealing the bound probes do not penetrate into the tissue. Instead, all surface silver labelling was assessed, and all immunopositive neurons throughout the depth of the selected sections were included. Quantification of the co-expression of different markers was determined as follows: first, neurons that showed the DAB-brown precipitate in the soma and primary dendrites were considered positive and counted. Second, neurons showing dense accumulation of black silver granules that followed the shape of the cell soma and that covered more than 50% of the soma surface (as evaluated in random cases that were digitized and analysed using ImageJ) were considered positive and counted. Use of the 100× objective provided an optimal resolution to identify double-positive neurons, even in cases where silver granules covered most of the soma surface, but not the proximal dendrites. Double-positive cases were confirmed by removing the silver granules (as described in Wang & Morales, 2009, and shown in Fig. 4). As the silver granules are formed in the photographic emulsion above the sections, neurons that were further away from the surface may produce false-negatives. However, the sum of the double-positive CBP/GABAergic neurons with the double-positive CBP/glutamatergic neurons accounted for nearly 100% of the CBP-immunopositive neurons in each case, indicating that the number of false-negatives is low.

Statistics

A normality test (Shapiro–Wilk, W) was used to assess the distribution of soma sizes of calbindin- and calretinin-positive neurons, and the Mann–Whitney rank sum (U) test was used to determine the difference in soma size between them (non-parametric statistics were used when one set or both sets of data to be compared failed normality). To
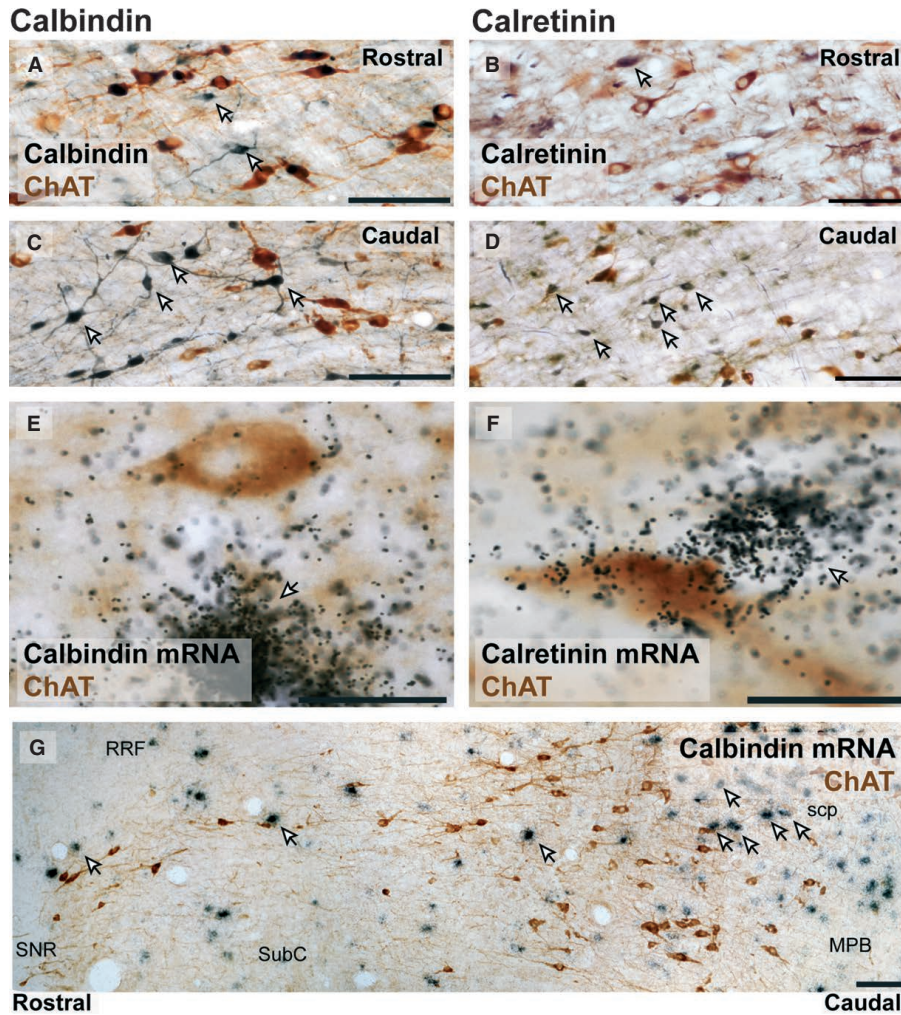
FIG. 1. Calbindin- and calretinin-positive neurons are present and widely distributed in the PPN. (A–G) Light micrographs of PPN sections that were double labelled to reveal ChAT (DAB brown precipitate) and calbindin (A, C) or calretinin (B, D), by IHC or *in situ* hybridization. (A, B) In the rostral PPN, calbindin- and calretinin-positive neurons (arrows) were sparse. (C, D) In contrast, in the caudal PPN the calbindin- and calretinin-positive neurons (arrows) were more abundant. (E–G) *In situ* hybridization combined with IHC was used to observe the presence and distribution of calbindin and calretinin mRNAs (black silver granules) within the PPN (ChAT staining shown as a DAB brown precipitate). Arrows indicate neurons positive for *in situ* hybridization signal. MPB, medial parabrachial nucleus; RRF, retrorubral field; scp, superior cerebellar peduncle; SNR, substantia nigra pars reticulata; SubC, subcoeruleus nucleus. Scale bars: A–D, G: 100 μm; E, F: 20 μm.

determine whether the total number of calbindin- and calretinin-positive neurons in the PPN were different, we used an unpaired *t*-test (*t*). To identify statistical differences in the distribution of calbindin- and calretinin-positive neurons (alone or co-expressing GAD65/67 or VGluT2 mRNA) across the rostro-caudal axis of the PPN, a one-way ANOVA (*F*, if data were normally distributed) or an ANOVA on ranks analysis (*H*, if data were not normally distributed) were used. To identify differences between segments (S1–S10), Tukey or Bonferroni and Dunn's *post hoc* tests were used for parametric and non-parametric data, respectively. The significance level for all tests was taken to be $P < 0.05$. Data are expressed as mean ± standard error of the mean (SEM) unless otherwise indicated.

Results

Presence of calcium binding proteins in the PPN

Neurons showing immunoreactivity for calbindin, calretinin and parvalbumin, identified by the grey precipitate, were observed within the borders of the PPN as defined by the neurons showing immunoreactivity for ChAT (brown DAB precipitate). Both calbindin and calretinin were observed to be widespread across all sections in which the PPN was contained. In contrast, parvalbumin-positive cell bodies were only observed in the most rostral segments of the most lateral PPN section of each brain containing the PPN. Furthermore, a large number of parvalbumin-positive fibres were strongly labelled across all PPN levels, hampering quantification of cell bodies. Given their low number, parvalbumin neurons were not included in further analyses.

Morphological properties of calbindin- and calretinin-positive neurons in the PPN

The calbindin-positive neurons were round, multipolar or bipolar in shape (Fig. 1A and C). The majority of these neurons were small, with a soma diameter of 14.5 ± 3.5 μm (mean ± SD; $n = 100$) that did not follow a normal distribution (Fig. 2A). Calbindin-positive neurons were found throughout the medio-lateral and rostro-caudal extent of
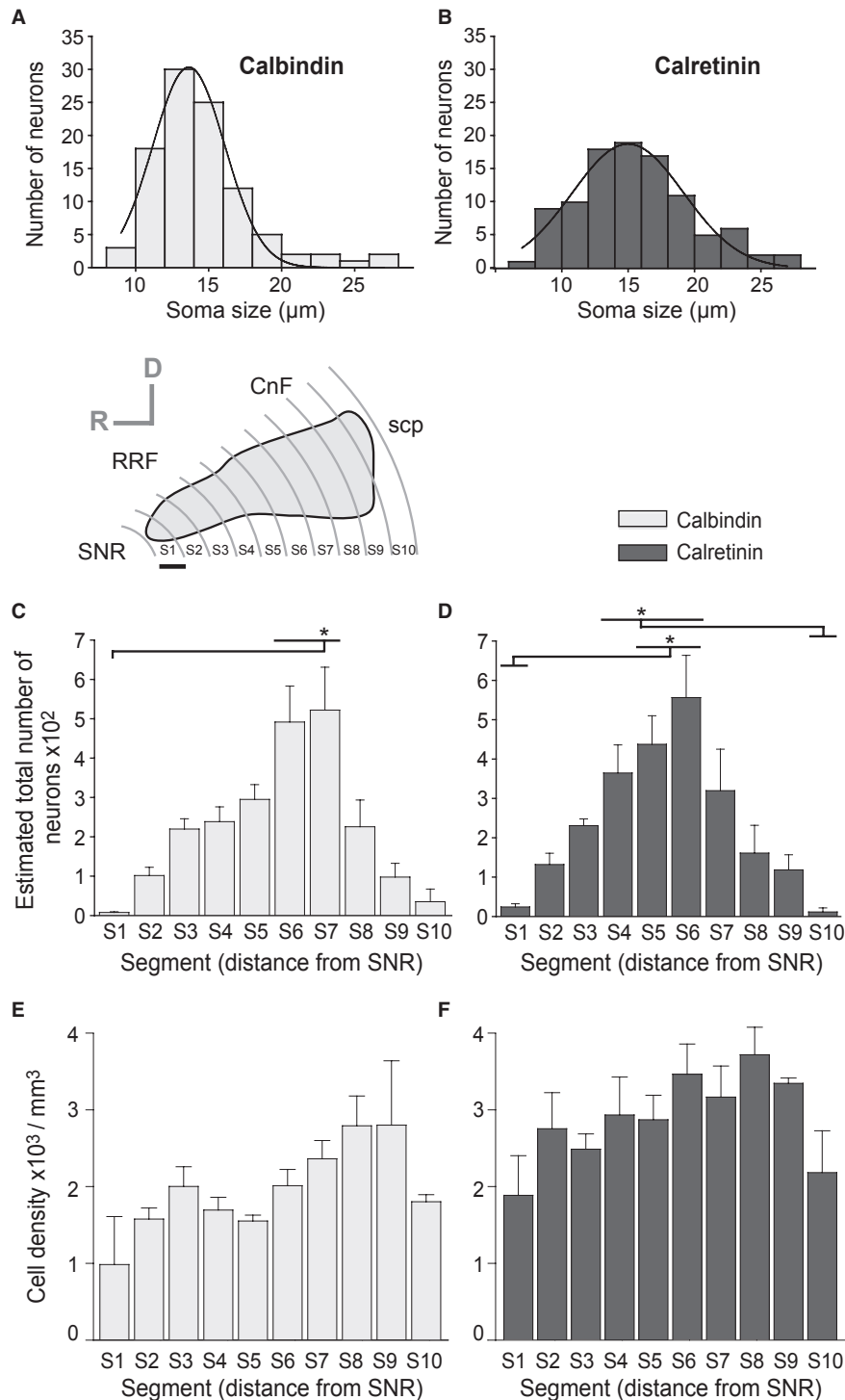
FIG. 2. Dimensions and distribution of calbindin- and calretinin-positive neurons in the PPN. (A, B) Distributions of cell body sizes of calbindin-positive ($n = 100$) and calretinin-positive ($n = 100$) neurons in the PPN. Calretinin-positive neurons are significantly larger than calbindin-positive neurons. (C, D) Estimated total number of calbindin- and calretinin-positive neurons according to a rostro-caudal segmentation of the PPN (S1–S10; $n = 6$; error bars indicate SEM) in the sagittal plane shown in the inset (10 segments S1–S10; scale: 300 μm). Segments in the caudal PPN show the largest number of neurons (see statistical details in text). (E, F) Average cell density of calbindin- and calretinin-positive neurons in the PPN. Both calbindin- and calretinin-positive neurons have a higher density in the caudal PPN than in the rostral PPN. CnF, cuneiform nucleus; D, dorsal; R, rostral; RRF, retrorubral field; scp, superior cerebellar peduncle; SNR, substantia nigra pars reticulata. *$P < 0.05$.

the PPN and were intermingled with cholinergic neurons. They were more abundant in the caudal part of the PPN (Fig. 1C) and did not follow the typical layer-like array distribution displayed by the cholinergic neurons (Fig. 1A, C and G).

The calretinin-positive neurons were irregular, multipolar or bipolar in shape (Fig. 1B and D), and varied in size from small to medium (diameter – 15.5 ± 4.4 μm, mean ± SD; $n = 100$), following a normal distribution ($W = 0.984$, $P = 0.264$; Fig. 2B). The calretinin-positive

neurons were significantly larger than the calbindin-positive neurons ($U = 4147$, $P = 0.037$). Similar to calbindin neurons, they were more densely concentrated in the caudal PPN (Fig. 1D).

We then tested for the presence of mRNAs for calbindin and calretinin in the PPN. Calbindin or calretinin mRNA was detected using a radioactive antisense probe in sections that were immunolabelled for ChAT neurons. Neurons with an accumulation of silver granules overlying them were considered positive for calbindin or calretinin mRNA, as appropriate (Fig. 1E and F). Similar numbers and rostro-caudal organization of calbindin- and calretinin-positive neurons were observed in the PPN by *in situ* hybridization as with IHC (Fig. 1E–G).

Distribution analysis and quantification of calbindin and calretinin neurons in the PPN

The calbindin- and calretinin-positive neurons were distributed across the whole extent of the PPN. The estimated number of neurons for both of these markers showed highest values in the middle segments of the PPN (S6 and S7 for calbindin and S5 and S6 for calretinin). An ANOVA on ranks analysis revealed that the differences in their distributions across PPN segments were significant (Kruskal–Wallis, $H = 37.77$ for calbindin and $H = 35.48$ for calretinin; $P < 0.001$; Fig. 2C and D; $n = 6$). A pairwise multiple comparisons Dunn's test between segments indicated that calbindin-positive neurons are more abundant in segments S6 and S7 than in segment S1 ($P < 0.05$; Fig. 2C), and that calretinin-positive neurons are more abundant in segments S5 and S6 than in segments S1 and S10, and in segment S4 than in segment S10 ($P < 0.05$; Fig. 2D). Although there were differences in cell densities, both calbindin- and calretinin-positive neurons showed a similar rostro-caudal variation in density, showing a higher density in the caudal segments than in the rostral segments of the PPN (Fig. 2E and F). The distribution of calbindin-positive neuron densities across segments was statistically different (ANOVA on ranks, $H = 19.51$; $P = 0.021$), but pairwise multiple comparisons between segments did not show specific differences (Fig. 2E). In contrast, a one-way ANOVA analysis indicated that there are no significant differences in the densities of calretinin-positive neurons (Fig. 2F).

The total number of calbindin-positive neurons in the PPN was 2318 ± 388 ($n = 6$) and the total number of calretinin-positive neurons was 2452 ± 408 ($n = 6$). The difference between the two populations was not significant ($P = 0.816$). Their numbers were slightly below the number of cholinergic neurons previously reported (2942 ± 122; Mena-Segovia *et al.*, 2009), but of a similar magnitude (neither was significantly different from the number of ChAT neurons), which suggested the possibility of some overlap between these three populations.

Co-localization of calcium-binding proteins with ChAT

To determine whether calbindin- or calretinin-positive neurons represent subpopulations of cholinergic neurons, we performed immunolabelling for ChAT in combination with immunolabelling (Fig. 3A′) or *in situ* hybridization (Fig. 1E and F) for calbindin and calretinin. Calbindin immunoreactivity was virtually non-existent in ChAT-positive neurons (Fig. 3A; estimated number of ChAT/calbindin double-positive neurons per animal – 4.2/4.2; $n = 2$). A slightly greater number was detected by *in situ* hybridization (Fig. 3B; number of ChAT/calbindin double-positive neurons per animal: 4/29; $n = 2$), possibly as a result of the higher sensitivity of the technique, but still representing only a small proportion of calbindin-positive neurons. The cell density of the ChAT/calbindin double-positive neurons was homogeneously distributed along the rostro-caudal axis of the PPN (Fig. 3B).

In contrast to calbindin, a larger proportion of calretinin-positive neurons were also immunoreactive for ChAT (Fig. 3A; 307 ± 104 ChAT/calretinin double-positive neurons; $n = 4$) and a similar degree of co-localization was identified by the combination of *in situ* hybridization and IHC (Fig. 3B; average number of ChAT/calretinin double-positive neurons per animal – 83/159; $n = 2$). Furthermore, and in contrast to ChAT/calbindin double-positive neurons, ChAT/calretinin double-positive neurons showed a heterogeneous, rostro-caudal distribution, with a larger number of neurons in the caudal portion of the PPN (Fig. 3B).

We then analysed the triple co-expression of ChAT, calbindin and calretinin by using immunofluorescence. No neurons were detected that co-expressed the three markers; however, we observed a large number of neurons co-expressing both CBPs (Fig. 3C; 23.9% of the total of calbindin-positive neurons and 24.8% of the total of calretinin-positive neurons; $n = 3$). Consistent with the findings of IHC and *in situ* hybridization, ChAT/calbindin double-positive neurons were not detected by this method and 5.3% of calretinin-positive neurons were also positive for ChAT.

VGluT2 and GAD65/67 mRNAs are present in calbindin and calretinin neurons in the PPN

To further characterize the nature of the calbindin- and calretinin-positive neurons, we combined a permanent IHC reaction for calbindin and calretinin with *in situ* hybridization for GAD65/67 or VGluT2 mRNA using radioactive antisense probes. We detected the mRNA for GAD65/67 and VGluT2 alone or associated with immunolabelling for calbindin and calretinin across all mediolateral and rostro-caudal levels of the PPN (Fig. 4). Positive neurons for both IHC and *in situ* hybridization were then counted in sagittal sections following the rostro-caudal segmentation of the PPN.

Consistent with previous reports (Mena-Segovia *et al.*, 2009; Wang & Morales, 2009), we observed that neurons expressing VGluT2 mRNA and GAD65/67 mRNA were similarly abundant in the PPN and have distinct distributions across the rostro-caudal axis of the PPN, GABAergic neurons being more concentrated in the rostral PPN and glutamatergic neurons more concentrated in the caudal PPN. Quantitative analysis showed that about one-third of the calbindin-positive neurons were also positive for GAD65/67 mRNA (38.5%) and thus GABAergic (Fig. 5A; 749 GAD65/67/calbindin double-positive neurons out of 1947 calbindin-positive neurons), and about two-thirds were positive for VGluT2 mRNA (66.5%) and thus glutamatergic (Fig. 5B; 1196 VGluT2/calbindin double-positive neurons out of 1798 calbindin-positive neurons). We then analysed the distribution of double-positive neurons across the rostro-caudal extent of the PPN (Fig. 5C–F). An ANOVA revealed that the distribution of the total number of GAD65/67mRNA/calbindin double-positive neurons was statistically different ($F_{9,17} = 3.214$, $P = 0.018$) but a pairwise multiple comparisons test (Bonferroni) was unable to identify differences between specific segments (Fig. 5C). To determine whether the differences in the distribution of neurons were a function of the change in volume, we analysed the density of neurons across segments. We observed a significant effect of the distribution (one-way ANOVA, $F_{9,17} = 3.458$, $P = 0.013$). A Tukey *post hoc* test showed that segment S3 had a significantly higher density of GAD65/67mRNA/calbindin double-positive neurons than segments S6, S7, S9 and S10 ($P = 0.042, 0.047, 0.03$ and 0.015, respectively;
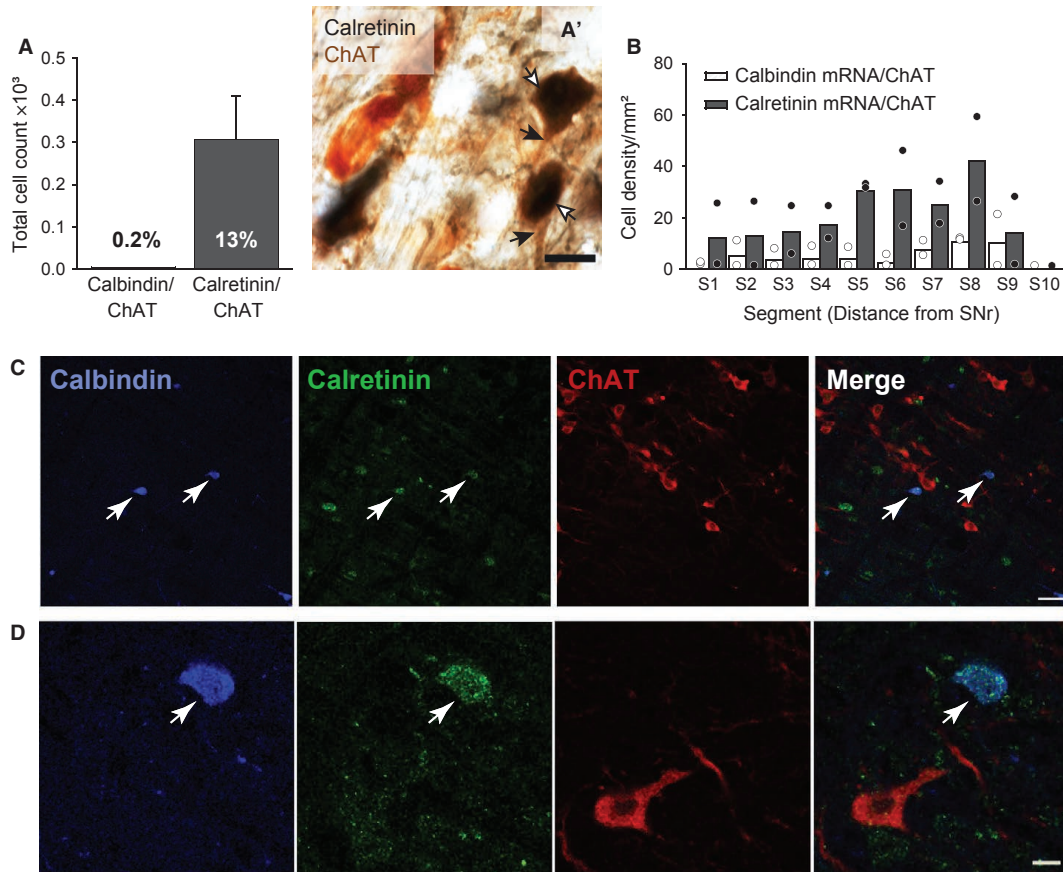
FIG. 3. Numbers and distribution of cholinergic neurons that express calcium-binding proteins in the PPN. (A) Total cell count for ChAT/calbindin (n = 2) and ChAT/calretinin (n = 4) double-positive neurons in the PPN. A double-positive neuron for ChAT and calretinin is shown in A' (white arrows show double-positive cell bodies and black arrows show brown dendrites, indicative of the DAB precipitate associated with ChAT labelling). (B) Distribution of cholinergic neurons that co-express calcium binding proteins following *in situ* hybridization for calbindin and calretinin mRNA. Data are expressed as the density of neurons (n = 2; bars show average, circles show individual values) across the rostro-caudal axis of the PPN (segments defined as S1–S10). (C, D) Low- and high-magnification images from triple immunoflourescent labelling for calretinin (green), calbindin (purple) and ChAT (red). In this example, immunoreactivity for calretinin co-localizes with immunoreactivity for calbindin (white arrow) but not with immunoreactivity for ChAT (merged image on the right). Scale bars: A' and D: 10 μm; C: 50 μm.

Fig. 5E). Similarly, the distribution of VGluT2/calbindin double-positive neurons was also significantly different across segments (ANOVA on ranks, $H = 20.024$, $P = 0.018$; Fig. 5D), and no differences between specific segments were found (Dunn's test). The density distribution also had a significant effect (one-way ANOVA, $F_{9,18} = 5.509$, $P = 0.001$), showing higher densities in segments S9 and S10 than in segments S1–S6 ($P = 0.038$, 0.007, 0.031, 0.01, 0.023 and 0.02 for S9, and 0.041, 0.01, 0.038, 0.014, 0.029 and 0.025 for S10, respectively; Fig. 5F).

Analysis of the calretinin-positive neurons revealed that 28.7% were also positive for GAD65/67 mRNA, and thus GABAergic (Fig. 6A; 701 GAD65/67/calretinin double-positive neurons out of 2499 calretinin-positive neurons). In contrast, 73.1% of the calretinin-positive neurons were also positive for VGluT2 mRNA, and thus glutamatergic (Fig. 6B; 1852 VGluT2/calretinin double-positive neurons out of 2534 calretinin-positive neurons). The distribution of calretinin double-positive neurons across the PPN was similar to that of calbindin double-positive neurons (Fig. 6C–F). In relation to the total number of calretinin/GAD65/67 double-positive neurons, their distribution was statistically different across PPN segments (one-way ANOVA, $F_{9,20} = 12.912$, $P < 0.001$), with segments S3–S5 showing significantly larger numbers than segment S10 ($P = 0.045$, 0.003 and 0.002, respectively), segments S4–S7 larger than segment S1

($P = 0.004$, 0.03, < 0.001 and < 0.001, respectively), segments S6 and S7 larger than S2, S8, S9 and S10 ($P = 0.008$, < 0.001, 0.003 and < 0.001 for S6, and 0.008, < 0.001, 0.003 and < 0.001 for S7, respectively) and segment S5 larger than S8 and S9 ($P = 0.014$ and 0.045, respectively; Bonferroni test; Fig. 6C). The density distribution of GAD65/67/calretinin-positive neurons was not significantly different (Fig. 6E). The distribution of the total number of calretinin/VGluT2 double-positive neurons was also statistically different across segments (one-way ANOVA, $F_{9,20} = 28.31$, $P < 0.001$), with segments S5–S7 showing significantly larger numbers than segments S1, S2, S3, S8, S9 and S10 ($P = < 0.001$, < 0.001, 0.006, 0.034, 0.006 and 0.002 for S5, and < 0.001 for all comparisons with S6 and S7), and segments S6 and S7 also larger than S4 ($P < 0.001$; Bonferroni test; Fig. 6D). The density distribution of VGluT2/calretinin double-positive neurons was significantly different (one-way ANOVA, $F_{9,20} = 3.852$, $P = 0.006$), with a Tukey *post hoc* test revealing differences in segment S10 compared with segment S2 ($P = 0.037$; Fig. 6F).

Discussion

The results of the present study provide a neurochemical and topographical characterization of the different types of neurons in
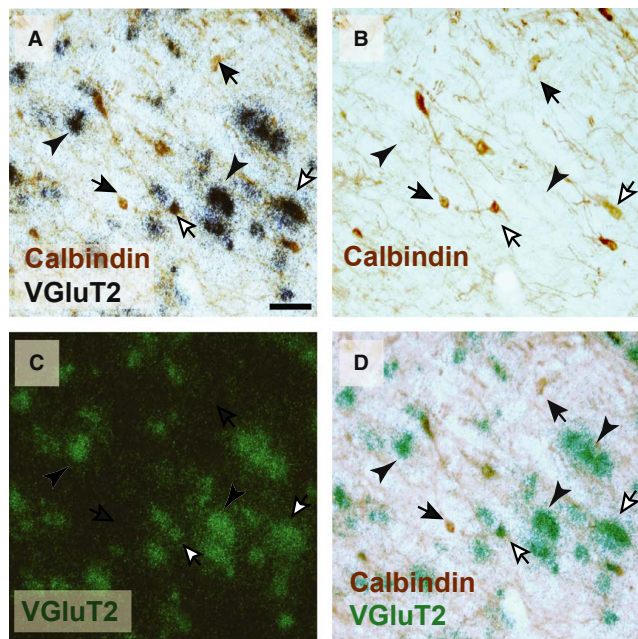
FIG. 4. VGlut2 mRNA is present in calbindin-positive neurons. (A–D) To confirm the expression and reliable visualization of VGluT2 mRNA (and GAD mRNA, image not shown) in sections that were previously treated for IHC for calbindin (A) and calretinin (image not shown), the black silver granules were removed in some sections (B) after obtaining epiluminescent images (C; VGlut2 mRNA as green grain aggregates). While the silver granules appear black under bright-field microscopy (A), they appear as green grains under epifluorescence (C, D). Bright-field and epiluminescent images (B, C) were then overlapped to confirm that a similar level of co-detection was observed with and without black silver granules removal. Scale bar: 50 μm.

the PPN. We report the presence of two CBPs, calbindin and calretinin, in all three types of PPN transmitter-defined neurons, i.e. cholinergic, GABAergic and glutamatergic neurons. The expression of these proteins identifies subclasses of the principal types of PPN neurons that may contribute differently to the functional properties of the PPN. Moreover, their differential distribution across the rostro-caudal extent of the PPN further supports a functional dichotomy between the rostral and the caudal portions of the nucleus (Mena-Segovia *et al.*, 2008b, 2009; Winn, 2008). Our findings thus provide new insight into the neuronal and topographical heterogeneity of the PPN.

Neuronal subtypes in the PPN

Cholinergic neurons in the PPN have been traditionally used to define the borders of the PPN (Mesulam *et al.*, 1983). Within these cholinergic borders, a large number of GABAergic and glutamatergic neurons have also been identified (Clements & Grant, 1990; Ford *et al.*, 1995), which are largely independent of each other and of the cholinergic neurons (Wang & Morales, 2009), and are heterogeneously distributed across different levels of the PPN (Mena-Segovia *et al.*, 2009). Nevertheless, characterization of the functional properties of cholinergic neurons has identified functional subpopulations. For instance, distinct membrane properties have been reported in cholinergic neurons from *in vitro* experiments: the majority of them produce A-type current under voltage clamp conditions (about 80%), but a small proportion also show low-threshold spikes or combined low-threshold spikes and A-current (Saitoh *et al.*, 2003). *In vivo*

experiments have revealed two distinct types of cholinergic neurons; those that are slow-firing and coupled to phasic increases in cortical fast frequency oscillations during sleep (about 80%), and those that are fast firing and coupled to the down-state of the cortical slow oscillations (Mena-Segovia *et al.*, 2008a). Whether the *in vitro* classification is correlated to the *in vivo* classification remains to be established, but interestingly, we revealed that about 10% of cholinergic neurons co-express calretinin. Further studies are required to determine whether calretinin-positive cholinergic neurons show distinct membrane and firing properties from calretinin-negative cholinergic neurons.

In contrast to cholinergic neurons, the non-cholinergic neurons (i.e. GABAergic and glutamatergic) are less well characterized, possibly due to the difficulty in unequivocally identifying molecular subtypes. Recent evidence points towards distinct functional roles among non-cholinergic neurons (Boucetta & Jones, 2009; Ros *et al.*, 2010), but no clear correlation with the GABAergic and glutamatergic phenotypes (or subphenotypes) has been obtained. The results presented here show that about one-third of both calbindin- and calretinin-positive neurons are GABAergic (38.5 and 28.7%, respectively), and two-thirds are glutamatergic (66.5 and 73.1%, respectively; data obtained from adjacent serial sections). As GABAergic and glutamatergic neurons are similar in overall numbers (Wang & Morales, 2009), this indicates that there is a larger proportion of glutamatergic neurons that express CBPs, compared with GABAergic neurons. Furthermore, the complementary proportions of calretinin- or calbindin-positive neurons that express GAD65/67 and VGluT2 mRNAs (totalling close to 100%) suggest that a large majority of CBP-expressing neurons are GABAergic or glutamatergic, with possibly the only exception being the 10% of cholinergic neurons that co-express calretinin. These findings indirectly suggest that it is unlikely that any other major population of neuron exists in the PPN. Moreover, the complementary figures also indicate that the calbindin/calretinin double-positive neurons are most likely to have a GABAergic or glutamatergic phenotype.

As seen in many other neuronal systems, such as the cortex, hippocampus and basal ganglia, the presence and type of CBP expressed by a particular type of neuron is correlated with specific functional properties. Previous reports showed that CBPs are present in the PPN, including calbindin, calretinin and parvalbumin (Dun *et al.*, 1995). In addition to calbindin and calretinin, in pilot studies we also evaluated the presence of parvalbumin in the PPN and observed that the number of positive neurons was very low compared with the other CBPs and restricted to the most rostral segments of the PPN. Even though they do not represent a major subtype of neuron in the PPN, in contrast to calbindin- and calretinin-positive neurons, future studies should aim to define their role in the neuronal organization of the PPN. It remains to be established whether neurons expressing CBPs have distinct physiological properties, but the findings here suggest the existence of subclasses of both GABAergic and glutamatergic neurons that might be associated with distinct functional properties. In support of this, two types of non-cholinergic PPN neuron with distinct discharge properties were found to form asymmetric synaptic contacts in their target structures (Mena-Segovia *et al.*, 2008a; Ros *et al.*, 2010). Because this type of synaptic contact is usually associated with excitatory synapses, it is likely that these functionally distinct neurons are glutamatergic, supporting the existence of different classes of neurons within this phenotype. Furthermore, in contrast to the basal forebrain where the majority of calbindin and calretinin neurons are putative glutamatergic neurons and only a small proportion are also immunoreactive for glutamic acid decarboxylase
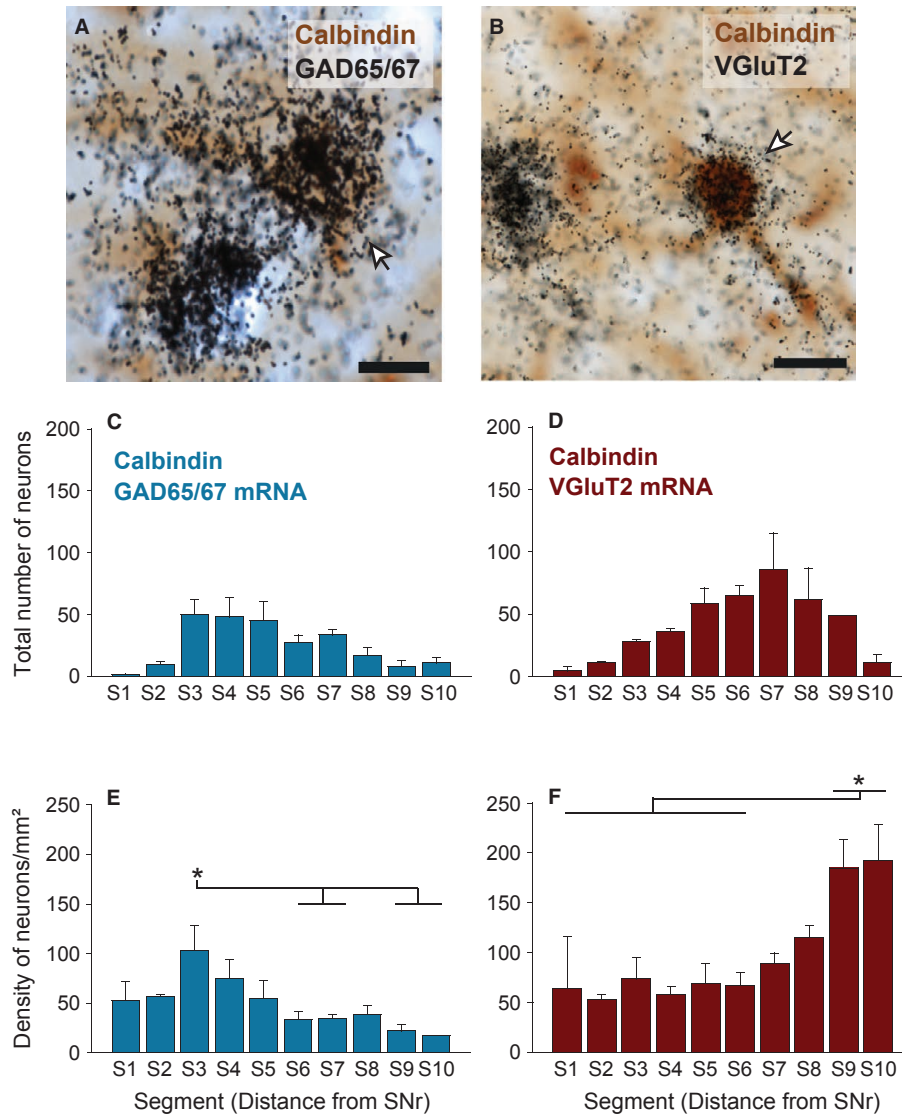
FIG. 5. Subpopulations of GABAergic and glutamatergic neurons that contain calbindin are present along the rostro-caudal axis of the PPN. (A, B) Light micrographs of PPN sections immunolabelled for calbindin (brown DAB precipitate) and labelled by *in situ* hybridization to reveal GAD65∕67 mRNA (A, dense accumulation of black silver granules) and VGluT2 mRNA (B). The neurons indicated by arrows express both corresponding markers. (C, D) Total number of GAD65∕67∕calbindin double-positive (C) and VGluT2∕calbindin double-positive (D) neurons in the PPN, showing significantly different distributions across rostro-caudal segments. (E, F) Average cell density of the GAD65∕67∕calbindin double-positive (E) and VGluT2∕calbindin double-positive (F) neurons in the PPN, also showing significantly different distributions ($n = 3$; error bars indicate SEM). Asterisks represent statistically different values (see text for detailed comparisons). Scale bar: 10 μm.

(Gritti *et al.*, 2003), the majority of neurons expressing GAD mRNA in the PPN also express CBPs, suggesting a highly heterogeneous GABAergic population in the PPN.

Internal subdivisions

All neuronal populations in the PPN are heterogeneously distributed across its rostro-caudal axis. GABAergic neurons are more densely concentrated in the rostral PPN (segments 1–5), whereas cholinergic and glutamatergic neurons are more densely concentrated in the caudal PPN (segments 6–10) (Fig. 1G; Mena-Segovia *et al.*, 2009). This same distribution holds true for cholinergic, GABAergic and gluta-matergic neurons that express CBPs. Thus, GABAergic neurons expressing calbindin or calretinin are more abundant in the rostral PPN, and glutamatergic neurons expressing calbindin or calretinin are

more abundant in the caudal PPN. These differences were more pronounced for calretinin-positive neurons, in which a higher proportion of VGluT2∕calretinin double-positive neurons were observed: in the rostral PPN the probability of a calretinin-positive neuron to be GABAergic or glutamatergic is nearly 1 : 1, whereas in the caudal PPN the probability to be glutamatergic is 4 : 1. These findings further support the notion of a neurochemical topography in the PPN.

The differential distribution of neurochemical subtypes in the PPN is closely correlated with the connectivity of the rostral and caudal portions of the nucleus (for a review see Martinez-Gonzalez *et al.*, 2011). Thus, the rostral PPN has close interconnectivity with the GABAergic output of the basal ganglia (SNr and internal globus pallidus∕entopeduncular nucleus) and the hypothalamus (e.g. Charara & Parent, 1994; Lavoie & Parent, 1994; Ford *et al.*, 1995). As the
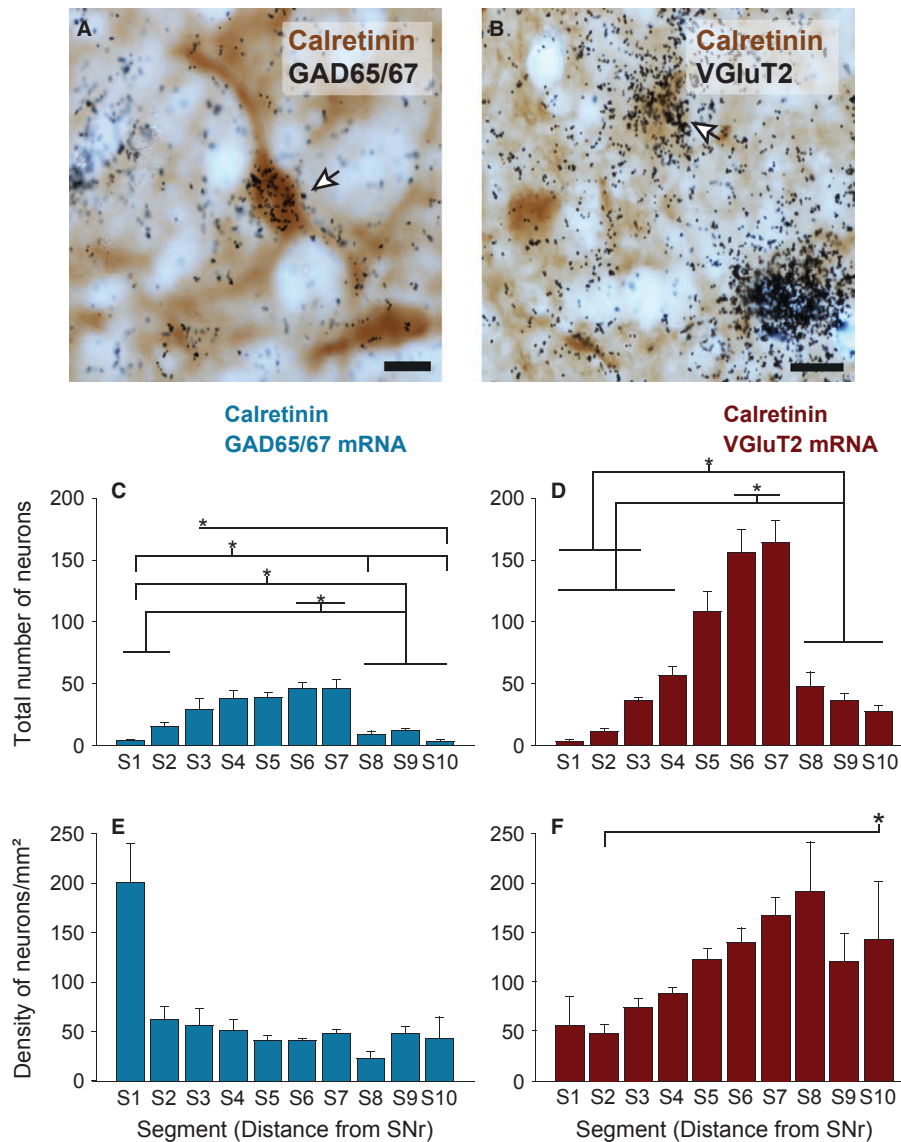
FIG. 6. Subpopulations of GABAergic and glutamatergic neurons that contain calretinin are topographically segregated in the PPN. (A, B) Light micrographs of PPN sections immunolabelled for calretinin (brown DAB precipitate) and labelled by *in situ* hybridization to reveal GAD65/67 mRNA (A, dense accumulation of black silver granules) and VGluT2 mRNA (B). The neurons indicated by arrows express both corresponding markers. (C, D) Total number of GAD65/67/calretinin double-positive (C) and VGluT2/calretinin double-positive (D) neurons in the PPN, showing significantly different distributions across rostro-caudal segments. Asterisks represent statistically different values (see text for detailed comparisons). (E, F) Average cell density revealing a significantly different distribution for VGluT2/calretinin double-positive (E) but not for GAD65/67/calretinin double-positive (F) neurons in the PPN (n = 3; error bars indicate SEM). Scale bar: 10 μm.

majority of neurons in this region of the nucleus are GABAergic (Mena-Segovia *et al.*, 2009), this suggests the existence of a predominantly GABAergic feedback circuit between basal ganglia and rostral PPN that could be involved in motor functions. In contrast, the caudal PPN mainly projects to the thalamus, subthalamic nucleus, ventral tegmental area, and superior and inferior colliculi (e.g. Beninato & Spencer, 1986; Smith *et al.*, 1988; Steriade *et al.*, 1988; Oakman *et al.*, 1995; Motts & Schofield, 2009; Kita & Kita, 2010). The output of this projection is mainly cholinergic and glutamatergic, and neurons in this region of the PPN receive inputs from the cortex and dorsal raphe (e.g. Steininger *et al.*, 1997; Matsumura *et al.*, 2000). Thus, this predominantly excitatory output may be mediating the arousal functions of the PPN. The expression of CBPs in the projection neurons of the PPN might then be associated with specific

functions depending on the region of the PPN in which they are located.

Conclusion

The data presented here provide a unique detailed characterization of the distribution and neurochemical composition of neurons expressing CBPs in the PPN. Furthermore, we have identified novel subtypes of cholinergic, GABAergic and glutamatergic neurons based on the combination of neurochemical markers. The heterogeneous distribution of these neuronal subtypes strengthens the notion of the PPN as a functionally dichotomous structure. The functional properties that these neuronal subtypes express will probably be dependent on the neuronal systems they are connected with and the discharge properties

they possess. The identification of novel neuronal subtypes in the PPN is essential to integrate the cellular basis that underlies the wide variety of functions the PPN is involved in.

Acknowledgements

Abbreviations

ABC, avidin-biotin peroxidase complex; CBPs, calcium binding proteins; ChAT, choline acetyltransferase; DAB, diaminobenzidine; IHC, immunohistochemistry; NDS, normal donkey serum; PB, phosphate buffer; PBS, phosphate-buffered saline; PFA, paraformaldehyde; PPN, pedunculopontine nucleus; SNr, substantia nigra pars reticulata; SSC, standard sodium citrate.

References

Acsady, L., Halasy, K. & Freund, T.F. (1993) Calretinin is present in non-pyramidal cells of the rat hippocampus – III. Their inputs from the median raphe and medial septal nuclei. *Neuroscience*, **52**, 829–841.

Alderson, H.L., Latimer, M.P. & Winn, P. (2006) Intravenous self-administration of nicotine is altered by lesions of the posterior, but not anterior, pedunculopontine tegmental nucleus. *Eur. J. Neurosci.*, **23**, 2169–2175.

Alderson, H.L., Latimer, M.P. & Winn, P. (2008) A functional dissociation of the anterior and posterior pedunculopontine tegmental nucleus: excitotoxic lesions have differential effects on locomotion and the response to nicotine. *Brain Struct. Funct.*, **213**, 247–253.

Beninato, M. & Spencer, R.F. (1986) A cholinergic projection to the rat superior colliculus demonstrated by retrograde transport of horseradish peroxidase and choline acetyltransferase immunohistochemistry. *J. Comp. Neurol.*, **253**, 525–538.

Boucetta, S. & Jones, B.E. (2009) Activity profiles of cholinergic and intermingled GABAergic and putative glutamatergic neurons in the pontomesencephalic tegmentum of urethane-anesthetized rats. *J. Neurosci.*, **29**, 4664–4674.

Camp, A.J. & Wijesinghe, R. (2009) Calretinin: modulator of neuronal excitability. *Int. J. Biochem. Cell Biol.*, **41**, 2118–2121.

Celio, M.R. (1990) Calbindin D-28k and parvalbumin in the rat nervous system. *Neuroscience*, **35**, 375–475.

Charara, A. & Parent, A. (1994) Brainstem dopaminergic, cholinergic and serotoninergic afferents to the pallidum in the squirrel monkey. *Brain Res.*, **640**, 155–170.

Chard, P.S., Bleakman, D., Christakos, S., Fullmer, C.S. & Miller, R.J. (1993) Calcium buffering properties of calbindin D28k and parvalbumin in rat sensory neurones. *J. Physiol.*, **472**, 341–357.

Clements, J.R. & Grant, S. (1990) Glutamate-like immunoreactivity in neurons of the laterodorsal tegmental and pedunculopontine nuclei in the rat. *Neurosci. Lett.*, **120**, 70–73.

Coté, P.Y. & Parent, A. (1992) Calbindin D-28k and choline acetyltransferase are expressed by different neuronal populations in pedunculopontine nucleus but not in nucleus basalis in squirrel monkeys. *Brain Res.*, **593**, 245–252.

Dun, N.J., Dun, S.L., Hwang, L.L. & Forstermann, U. (1995) Infrequent co-existence of nitric oxide synthase and parvalbumin, calbindin and calretinin immunoreactivity in rat pontine neurons. *Neurosci. Lett.*, **191**, 165–168.

Ford, B., Holmes, C.J., Mainville, L. & Jones, B.E. (1995) GABAergic neurons in the rat pontomesencephalic tegmentum: codistribution with cholinergic and other tegmental neurons projecting to the posterior lateral hypothalamus. *J. Comp. Neurol.*, **363**, 177–196.

Fortin, M. & Parent, A. (1999) Calretinin-immunoreactive neurons in primate pedunculopontine and laterodorsal tegmental nuclei. *Neuroscience*, **88**, 535–547.

Garcia-Rill, E., Houser, C.R., Skinner, R.D., Smith, W. & Woodward, D.J. (1987) Locomotion-inducing sites in the vicinity of the pedunculopontine nucleus. *Brain Res. Bull.*, **18**, 731–738.

Garcia-Rill, E., Kinjo, N., Atsuta, Y., Ishikawa, Y., Webber, M. & Skinner, R.D. (1990) Posterior midbrain-induced locomotion. *Brain Res. Bull.*, **24**, 499–508.

Gritti, I., Manns, I.D., Mainville, L. & Jones, B.E. (2003) Parvalbumin, calbindin, or calretinin in cortically projecting and GABAergic, cholinergic, or glutamatergic basal forebrain neurons of the rat. *J. Comp. Neurol.*, **458**, 11–31.

Gulyas, A.I., Toth, K., Danos, P. & Freund, T.F. (1991) Subpopulations of GABAergic neurons containing parvalbumin, calbindin D28k, and chole-cystokinin in the rat hippocampus. *J. Comp. Neurol.*, **312**, 371–378.

Inglis, W.L., Olmstead, M.C. & Robbins, T.W. (2001) Selective deficits in attentional performance on the 5-choice serial reaction time task following pedunculopontine tegmental nucleus lesions. *Behav. Brain Res.*, **123**, 117–131.

Kita, T. & Kita, H. (2010) Cholinergic and non-cholinergic mesopontine tegmental neurons projecting to the subthalamic nucleus in the rat. *Eur. J. Neurosci.*, **33**, 433–443.

Kretsinger, R.H. & Nockolds, C.E. (1973) Carp muscle calcium-binding protein. II. Structure determination and general description. *J. Biol. Chem.*, **248**, 3313–3326.

Lavoie, B. & Parent, A. (1994) Pedunculopontine nucleus in the squirrel monkey: projections to the basal ganglia as revealed by anterograde tract-tracing methods. *J. Comp. Neurol.*, **344**, 210–231.

Martinez-Gonzalez, C., Bolam, J.P. & Mena-Segovia, J. (2011) Topographical organization of the pedunculopontine nucleus. *Front. Neuroanat.*, **5**, 22–31.

Matsumura, M., Nambu, A., Yamaji, Y., Watanabe, K., Imai, H., Inase, M., Tokuno, H. & Takada, M. (2000) Organization of somatic motor inputs from the frontal lobe to the pedunculopontine tegmental nucleus in the macaque monkey. *Neuroscience*, **98**, 97–110.

Mena-Segovia, J., Sims, H.M., Magill, P.J. & Bolam, J.P. (2008a) Cholinergic brainstem neurons modulate cortical gamma activity during slow oscillations. *J. Physiol.*, **586**, 2947–2960.

Mena-Segovia, J., Winn, P. & Bolam, J.P. (2008b) Cholinergic modulation of midbrain dopaminergic systems. *Brain Res. Rev.*, **58**, 265–271.

Mena-Segovia, J., Micklem, B.R., Nair-Roberts, R.G., Ungless, M.A. & Bolam, J.P. (2009) GABAergic neuron distribution in the pedunculopontine nucleus defines functional subterritories. *J. Comp. Neurol.*, **515**, 397–408.

Mesulam, M.M., Mufson, E.J., Wainer, B.H. & Levey, A.I. (1983) Central cholinergic pathways in the rat: an overview based on an alternative nomenclature (Ch1-Ch6). *Neuroscience*, **10**, 1185–1201.

Motts, S.D. & Schofield, B.R. (2009) Sources of cholinergic input to the inferior colliculus. *Neuroscience*, **160**, 103–114.

Nagerl, U.V., Novo, D., Mody, I. & Vergara, J.L. (2000) Binding kinetics of calbindin-D(28k) determined by flash photolysis of caged Ca^{2+}. *Biophys. J.*, **79**, 3009–3018.

Oakman, S.A., Faris, P.L., Kerr, P.E., Cozzari, C. & Hartman, B.K. (1995) Distribution of pontomesencephalic cholinergic neurons projecting to substantia nigra differs significantly from those projecting to ventral tegmental area. *J. Neurosci.*, **15**, 5859–5869.

Olszewski, J. & Baxter, D. (1982) *Cytoarchitecture of the Human Brain Stem*. S. Karger AG, Basel.

Pahapill, P.A. & Lozano, A.M. (2000) The pedunculopontine nucleus and Parkinson's disease. *Brain*, **123**, 1767–1783.

Parent, A., Fortin, M., Coté, P.Y. & Cicchetti, F. (1996) Calcium-binding proteins in primate basal ganglia. *Neurosci. Res.*, **25**, 309–334.

Pochet, R., Parmentier, M., Lawson, D.E. & Pasteels, J.L. (1985) Rat brain synthesizes two 'vitamin D-dependent' calcium-binding proteins. *Brain Res.*, **345**, 251–256.

Ros, H., Magill, P.J., Moss, J., Bolam, J.P. & Mena-Segovia, J. (2010) Distinct types of non-cholinergic pedunculopontine neurons are differentially modulated during global brain states. *Neuroscience*, **170**, 78–91.

Saitoh, K., Hattori, S., Song, W.J., Isa, T. & Takakusaki, K. (2003) Nigral GABAergic inhibition upon cholinergic neurons in the rat pedunculopontine tegmental nucleus. *Eur. J. Neurosci.*, **18**, 879–886.

Schwaller, B., Meyer, M. & Schiffmann, S. (2002) 'New' functions for 'old' proteins: the role of the calcium-binding proteins calbindin D-28k, calretinin and parvalbumin, in cerebellar physiology. Studies with knockout mice. *Cerebellum*, **1**, 241–258.

Skinner, R.D. & Garcia-Rill, E. (1984) The mesencephalic locomotor region (MLR) in the rat. *Brain Res.*, **323**, 385–389.

Smith, Y., Pare, D., Deschenes, M., Parent, A. & Steriade, M. (1988) Cholinergic and non-cholinergic projections from the upper brainstem core to the visual thalamus in the cat. *Exp. Brain Res.*, **70**, 166–180.

Staiger, J.F., Masanneck, C., Schleicher, A. & Zuschratter, W. (2004) Calbindin-containing interneurons are a target for VIP-immunoreactive synapses in rat primary somatosensory cortex. *J. Comp. Neurol.*, **468**, 179–189.

Steininger, T.L., Wainer, B.H., Blakely, R.D. & Rye, D.B. (1997) Serotonergic dorsal raphe nucleus projections to the cholinergic and noncholinergic

neurons of the pedunculopontine tegmental region: a light and electron microscopic anterograde tracing and immunohistochemical study. *J. Comp. Neurol.*, **382**, 302–322.

Steriade, M., Pare, D., Parent, A. & Smith, Y. (1988) Projections of cholinergic and non-cholinergic neurons of the brainstem core to relay and associational thalamic nuclei in the cat and macaque monkey. *Neuroscience*, **25**, 47–67.

Steriade, M., Datta, S., Pare, D., Oakson, G. & Curro Dossi, R.C. (1990) Neuronal activities in brain-stem cholinergic nuclei related to tonic activation processes in thalamocortical systems. *J. Neurosci.*, **10**, 2541–2559.

Vincent, S.R. & Kimura, H. (1992) Histochemical mapping of nitric oxide synthase in the rat brain. *Neuroscience*, **46**, 755–784.

Vincent, S.R., Satoh, K., Armstrong, D.M. & Fibiger, H.C. (1983) NADPH-diaphorase: a selective histochemical marker for the cholinergic neurons of the pontine reticular formation. *Neurosci. Lett.*, **43**, 31–36.

Wang, H.L. & Morales, M. (2008) Corticotropin-releasing factor binding protein within the ventral tegmental area is expressed in a subset of dopaminergic neurons. *J. Comp. Neurol.*, **509**, 302–318.

Wang, H.L. & Morales, M. (2009) Pedunculopontine and laterodorsal tegmental nuclei contain distinct populations of cholinergic, glutamatergic and GABAergic neurons in the rat. *Eur. J. Neurosci.*, **29**, 340–358.

Winn, P. (2008) Experimental studies of pedunculopontine functions: are they motor, sensory or integrative? *Parkinsonism Relat. Disord.*, **14**(Suppl 2), S194–S198.